

A PRECISE EXTRACTION OF $R = \sigma_L/\sigma_T$ FROM A GLOBAL ANALYSIS OF THE SLAC DEEP INELASTIC $e-p$ AND $e-d$ SCATTERING CROSS SECTIONS*

L. W. WHITLOW^a

Stanford University, Stanford, California 94305

S. ROCK

The American University, Washington, DC 20016

A. BODEK

University of Rochester, Rochester, New York 14627

E. M. RIORDAN and S. DASU

Stanford Linear Accelerator Center, Stanford, CA 94309

ABSTRACT

We report the extraction of $R = \sigma_L/\sigma_T$ from a global analysis of eight SLAC deep inelastic experiments on $e-p$ and $e-d$ scattering performed between 1970 and 1985. Values of R^p , R^d , and $R^d - R^p$ are determined over the entire SLAC kinematic range: $0.1 \leq x \leq 0.9$ and $0.6 \leq Q^2 \leq 20.0$ (GeV/c)². We find that $R^p = R^d$, as expected in QCD. Measured values of $R(x, Q^2)$ are larger than predictions based on perturbative QCD and on QCD with the inclusion of kinematic target mass terms, indicating that dynamical higher twist effects may be important in the SLAC kinematic range.

Submitted to *Physics Letters*

*This work was supported in part by Department of Energy contracts DE-AC03-76SF00515 and DE-AC02-76ER13065; by National Science Foundation Grant PHY85-10549; and by Lawrence Livermore National Laboratories-Stanford University Research Participation Agreement No. 6936905.

^aCurrent address: Stanford Linear Accelerator Center, Stanford University, Stanford, CA 94309.

Since 1970 a series of eight deep inelastic e - p and e - d scattering experiments^{1–8} at SLAC has steadily improved our knowledge of the proton and deuteron structure functions. The most recent of these, known as E140,⁸ was a high precision experiment designed to extract $R = \sigma_L/\sigma_T$ from deep inelastic e - d and e - Fe cross sections. The results of this experiment proved to be larger than predictions⁹ based on perturbative QCD (R^{QCD}) and on QCD with the inclusion of kinematic target ‘mass effects’ ($R^{\text{QCD+TM}}$), suggesting that dynamical higher twist effects might play an important role in nucleon structure in the SLAC kinematic range.

Besides comparisons of this ratio with theoretical predictions, accurate values of $R(x, Q^2)$ are needed for extracting structure functions from deep inelastic lepton-nucleon scattering cross sections. For lack of better information, constant values (e.g., $R = 0$ at CERN or $R = 0.18$ at SLAC) have typically been assumed in extracting structure functions.

Two previous attempts^{4,6} to extract R from a combined analysis of several SLAC experiments met with only partial success. The accuracy of the extracted values was limited primarily by large uncertainties in the radiative corrections and in the relative normalizations of the various experiments included in these analyses.

We report here new extractions¹¹ of R^p , R^d , and $R^d - R^p$ from a combined re-analysis of 5835 deep inelastic e - p and e - d cross section measurements, each with typically $\pm 3\%$ statistical accuracy, from eight experiments using the 1.6 GeV, 8 GeV, and 20 GeV spectrometers at the SLAC End Station A facility.¹² Our analysis benefits from three major analytical advances: a new radiative corrections procedure that reduces the corresponding systematic error in $R(x, Q^2)$ to the level of ± 0.025 ; a much more accurate method of mutually normalizing the eight datasets; and a detailed propagation of systematic errors that exploits all known correlations and results in smaller, more accurate estimates of the systematic uncertainty

in R . Extractions of $R(x, Q^2)$ are made over the kinematic range: $0.1 \leq x \leq 0.9$ and $0.6 \leq Q^2 \leq 20.0$ (GeV/c)².

In the first Born approximation, the deep inelastic electron-nucleon scattering cross section can be written in terms of the two structure functions F_1 and F_2 as

$$\frac{d^2\sigma}{d\Omega dE'} = \frac{4\alpha^2 E'^2}{Q^4} \left[\frac{1}{\nu} F_2(x, Q^2) + \frac{2}{M} F_1(x, Q^2) \tan^2\left(\frac{\theta}{2}\right) \right], \quad (1)$$

where $Q^2 = 4EE' \sin^2(\frac{\theta}{2})$ is the invariant four-momentum transfer, E is the energy of the incident electron, θ the scattering angle, and E' the final electron energy in the lab frame, M is the nucleon mass, $\nu = E - E'$ is the energy transfer, and $x = Q^2/2M\nu$ is the Bjorken scaling variable. This cross section can also be expressed in terms of

$$R = \frac{F_2}{2xF_1} \left(1 + \frac{4M^2 x^2}{Q^2} \right) - 1 \quad (2)$$

and σ_T , the cross section for absorption of transversely polarized virtual photons, as

$$\frac{d^2\sigma}{d\Omega dE'} = \Gamma \sigma_T(x, Q^2) [1 + \epsilon R(x, Q^2)], \quad (3)$$

where

$$\Gamma = \frac{\alpha E'}{4\pi^2 M E} \left(\frac{1}{x} - \right) \frac{1}{1 - \epsilon} \quad (4)$$

is the virtual photon flux with polarization given by $\epsilon = [1 + (1 + \nu^2/Q^2) \tan^2(\frac{\theta}{2})]^{-1}$.

As indicated in eq. (3), the extraction of R requires cross section measurements over a span in ϵ for a given value of (x, Q^2) .

We began the global analysis by correcting¹¹ all cross sections for radiative effects according to the Bardin/Tsai prescription.^{11,13} The “internal” portion of these corrections was calculated using the exact prescription of Akhundov, Bardin,

and Shumeiko.¹⁴ The “external” portion (due to straggling of the electrons in the target material) was calculated according to the formulation of Tsai,¹⁵ using detailed models of the targets employed in each experiment. Comparisons with the previous SLAC radiative corrections procedure¹⁶ show typical differences of several percent, and of up to 5% at $x \leq 0.2$.

The uncertainty in the internal radiative correction was evaluated by comparison with an improved version of the “exact” formalism of Tsai.¹⁷ There is excellent agreement between these two formulations¹³ with some noteworthy differences, in particular, correlated with ϵ but not with x or Q^2 . This c -correlated uncertainty propagates through eq. (3) into an uncertainty in R of ± 0.025 . In addition, we estimate an overall (uncorrelated) uncertainty of $\pm 1\%$, which is included in the overall normalization uncertainty but does not contribute to the uncertainty in R . The uncertainty in the external radiative correction was estimated to be negligible¹³ from comparisons of cross sections measured on targets with different thicknesses.^{7,8} Additional uncertainties due to the structure function parameterizations used to calculate the radiative corrections were evaluated¹¹ in an iterative fashion and are negligible for $x > 0.1$ and $Q^2 > 1.0$ (GeV/c)².

The data of the other seven experiments were normalized” to those of E140 by fitting all cross section measurements to a smooth model with floating normalization parameters for each experiment. The best fit normalizations, N_i , relative to E140, are shown in table 1 with statistical and systematic uncertainties. The systematic errors give the estimated dependence of N_i on model choice and on various kinematic cuts. The one exception to this procedure is the normalization of the E89a data, which are kinematically disjoint from those of the other experiments. For E89a the normalization factor was determined using comparisons¹¹ of measured elastic cross sections with those of the other experiments. Except for

this case, the N_i are strongly correlated; accounting for these correlations greatly reduces the uncertainty in R due to the uncertainties in the N_i .

Not indicated in table 1 are the overall normalization uncertainties of the global analysis, which do not propagate into the error in R . For deuterium, this is exactly the E140 normalization uncertainty, $\pm 1.7\%$. By requiring that $N^p = N^d$ for E49b, we choose E49b as the normalization anchor for the hydrogen data. This choice introduces an additional $\pm 1.0\%$ uncertainty in the hydrogen normalization, yielding a total hydrogen normalization uncertainty of $\pm 2.1\%$.

These normalized cross sections were binned in intervals of x and Q^2 , and a bin-centering correction applied. To extract $R(x, Q^2)$ at the center of each bin, the cross section values were linearly regressed versus ϵ according to eq. (3). Statistical and systematic errors in the original cross sections were propagated through the regression analysis, respecting all known correlations. Each value of $R(x, Q^2)$ was typically extracted from six cross section measurements from four experiments spanning an ϵ range of 0.5. The average value of χ^2 per degree of freedom (χ^2/df) for these fits is 0.91, over a total of 176 separate regressions.

In a similar manner², we extracted $R^d - R^p$ by linearly regressing the deuterium/hydrogen cross section ratios versus $\epsilon' \equiv 1/(1+\epsilon R^p)$, where we use a model (see below) for R^p . These fits display an average value of χ^2/df of 0.99, over a total of 86 separate regressions. Because the extracted values of $R^d - R^p$ show no Q^2 dependence, they are averaged over Q^2 at each value of x . As illustrated in fig. 1, these averages are consistent with zero over the full range of x , in strong disagreement with predictions based on diquark formation. Averaging over the full kinematic range, we obtain

$$R^d - R^p = -0.001 \pm 0.009_{\text{stat}} \pm 0.009_{\text{syst}} , \quad (5)$$

from which we conclude that $R^p = R^d$, which also implies⁴ $R^n = R^p$. Such a strict equality places sharp constraints on any nonperturbative contributions to parton dynamics that require large differences between R^n and R^p .

In light of this result, we averaged¹⁹ the extracted R^p and R^d in each (x, Q^2) bin into a single value of R ; these data are presented in fig. 2. Because E140 measured R very accurately by itself, we have not included the E140 deuterium cross sections in the global extractions of R^d . Thus, the E140 results²³ shown in fig. 2 (which are averages of R^d and R^{Fe}) are independent of the combined global extractions of R . Numerical values of the global extractions of R^p , R^d , and R (and improved E140 extractions of R^d , R^{Fe} , and R) are given in ref. 11.

Also shown in fig. 2 are the high- Q^2 $\mu - N$ and $\nu - N$ scattering measurements of R from the EMC,²⁰ BCDMS,²¹ and CDHSW²² collaborations. The dotted and dashed curves represent calculations⁹ of R^{QCD} and¹⁰ $R^{\text{QCD+TM}}$ using quark distributions of CDHS,⁹ and the solid curve represents R^{fit} , a best-fit model to all the lepton-scattering data in fig. 2.

The global extractions of $R(x, Q^2)$ are in excellent agreement with the results of E140, except possibly near $x = 0.175$. The measured values of $R(x, Q^2)$ are systematically higher than R^{QCD} and $R^{\text{QCD+TM}}$ in the SLAC kinematic range. For the 100 SLAC (global plus E140) measurements, the χ^2 of these calculations are 465 and 207, respectively, and only 17 of these measurements fall below $R^{\text{QCD+TM}}$ (none by more than one standard deviation). This is evidence that, even with kinematic target mass effects included, perturbative QCD is an incomplete theory of nucleon structure in the SLAC kinematic range.

Such a discrepancy may be due to higher twist contributions to R , which are expected to be large at SLAC values of Q^2 and positive at leading order.

The observed z -dependence of R may be an important indicator of the dominant higher twist effects. In fig. 3 we present the SLAC data as a function of x , averaged over the range in Q^2 from 5 to 10 (GeV/c)². Also shown are several predictions for $R(x)$ and the best fit model (see below) evaluated at the mean Q^2 of 7 (GeV/c)².

Included in fig. 3 are the results of a recent phenomenological analysis²³ of the twist-4 contribution to R (which was based on our preliminary results for R^d). The predicted variation of R is in excellent agreement with our data ($\chi^2/df = 61/72$), although it is essentially limited to $x \leq 0.625$ and $Q^2 \geq 4.0$ (GeV/c)² by uncertainties in the parton distribution functions. Within the naïve quark-parton model, the magnitude of the twist-4 term that fits our data is consistent with what is expected for a primordial parton transverse momentum of 200 to 300 MeV/c.

Several authors have speculated^{18,24} that diquark formation may be an important factor in nucleon structure. As indicated in fig. 3, spin-0 diquark formation would generate a large contribution to R at high x and low Q^2 , in strong disagreement with our measurements of R .

Given our limited theoretical understanding of R , it is important to have a parameterization of $R(x, Q^2)$ that spans the entire kinematic range of deep inelastic scattering. The solid curve in figs. 2 and 3 represents a least-squares fit to all 139 lepton-scattering measurements of R shown in fig. 2:

$$R^{fit} = \frac{b_1}{\ln(Q^2/\Lambda^2)} \Theta(x, Q^2) + \frac{b_2}{Q^2} + \frac{b_3}{Q^4 + 0.3^2}, \quad (6)$$

where $\Lambda \equiv 0.2$ GeV, and

$$\Theta(x, Q^2) \equiv 1 + 12 \left(\frac{Q^2}{Q^2 + 1} \right) \left(\frac{0.125^2}{0.125^2 + x^2} \right) \quad (7)$$

gives the logarithmic term an x dependence that matches R^{QCD} at high Q^2 . This model fits the data with a χ^2 of 110, yielding best-fit parameters $b_1 = 0.635$,

$b_2 = 0.5747$, and $b_3 = -0.3534$. By design, R^{fit} extrapolates to theoretically reasonable values outside the kinematic range of the data: inside the resonance region; as $x \rightarrow 0$ and 1; and as $Q^2 \rightarrow \infty$. However, this model should not be used for $Q^2 \leq 0.3$ (GeV/c)². A convenient parameterization of the uncertainty in R^{fit} is provided in ref. 11.

In summary, we have shown that $R^p = R^d$ to high accuracy, and consequently that $R^n = R^p$. We observe that $R(x, Q^2)$ is larger than predictions based on QCD and on QCD with target mass effects. This disparity may be due to contributions from dynamical higher twist effects, a possibility supported by a recent phenomenological analysis of next-to-leading twist contributions. The extracted values of R and $R^d - R^p$ are not, however, consistent with predictions based on diquark formation. Lastly, we present a best fit parameterization of $R(x, Q^2)$ valid over the combined kinematic ranges of the SLAC and CERN deep inelastic lepton-scattering data. This fit has been used to extract precise values of the proton and deuteron structure functions from the SLAC data; this analysis will be presented in forthcoming publications.

We wish to thank SLAC Group A and the Spectrometer Facilities Group at SLAC for their assistance and for their excellent archival efforts.

REFERENCES

- [1] J. S. Poucher *et al.*, Phys. Rev. Lett. 32 (1974) 118; J. S. Poucher, Ph.D. thesis, Massachusetts Institute of Technology, MIT-LNS (1971); see also ref. 4.
- [2] E. M. Riordan, Ph.D. thesis, Massachusetts Institute of Technology, MIT-LNS RX-648 (1973); A. Bodek, Ph.D. thesis, Massachusetts Institute of Technology, MIT-LNS COO-3069-116 (1972); see also ref. 4.
- [3] S. Stein *et al.*, Phys. Rev. D11 (1975) 1884.
- [4] A. Bodek *et al.*, Phys. Rev. D21 (1979) 1471.
- [5] W. B. Atwood *et al.*, Phys. Lett. B64 (1976) 479; W. B. Atwood, Ph.D. thesis, Stanford University, SLAC-Report-185 (1975).
- [6] M. D. Mestayer *et al.*, Phys. Rev. D27 (1983) 285; M. D. Mestayer, Ph.D. thesis, Stanford University, SLAC-Report-214 (1978).
- [7] R. G. Arnold *et al.*, Phys. Rev. Lett. 52 (1984) 727; J.G. Gomez *et al.*, to be published; J.G. Gomez, Ph.D. thesis, The American University, (1987).
- [8] L. W. Whitlow, Ph.D. thesis, Stanford University, SLAC-Report-357 (1990).
This thesis improves upon the E140 results of two previous publications: S. Dasu *et al.*, Phys. Rev. Lett. 60, (1988) 2591; S. Dasu *et al.*, Phys. Rev. Lett. 61 (1988) 1061. See also ref. 13.
- [9] G. Alardisi and G. Martinelli, Phys. Lett. B76 (1978) 89; input quark distributions are from the CDHS collaboration, see B. Vallage, Ph.D. thesis, University de Paris-Sud, (1984).
- [10] H. Georgi and H. D. Politzer, Phys. Rev. D14 (1976) 1829; the calculations presented here supercede those of Refs. 8 and 12.
- [11] L. W. Whitlow, ref. 8.

[12] NPAS Users Guide, SLAC-Report-269 (1984); see also ref. 4.

[13] S. Dasu, Ph.D. thesis, University of Rochester, UR-1059 (1988).

[14] A. A. Akhundov *et al.*, Sov. J. Nucl. Phys. 44 (1986) 1212; D. Yu Bardin *et al.*, Nucl. Phys. B197 (1982) 1 and references therein.

[15] We follow closely Y. S. Tsai, SLAC-PUB-848 (1971) with two important modifications: we add μ , τ and quark loops to the vacuum polarization diagram; and we do not make the energy peaking approximation, instead evaluating the double integral over $[dE dE']$.

[16] Y. S. Tsai, Rev. Mod. Phys. 46 (1974) 815; Y. S. Tsai, ref. 15; L. W. MO and Y. S. Tsai, Rev. Mod. Phys. 41 (1969) 295.

[17] Starting with eq. A.24 of Y .S. Tsai, ref. 15, our procedure included the vacuum polarization correction of ref. 15; a correction for multiple soft-photon emission (this was used in the peaking approximation formulas but not in eq. A.24); and the numerical integration over the bremsstrahlung photon angle when the photon energy is less than the cutoff parameter A. See ref. 13 for details.

[18] S. Ekelin and S. Fredriksson, Phys. Lett. B162 (1985) 373.

[19] We respect the asymmetric parent distribution of the R measurements in the manner suggested by A. Bodek, SLAC-TN-74-2 (1974), a portion of which is available as Nucl. Instrum Methods 117 (1974) 613.

[20] J. J. Aubert *et al.*, Nucl. Phys. B259 (1985) 189; J. J. Aubert *et al.*, Nucl. Phys. B293 (1987) 740.

[21] A. C. Benvenuti *et al.*, Phys. Lett. B223 (1989) 485 ; A. C. Benvenuti *et al.*, CERN-EP/89-170 (1989), submitted to Phys. Lett. B.

[22] P. Berge *et al.*, CERN-EP/89-103 (1989), submitted to Z. Phys. C.

[23] J. L. Miramontes *et al.*, Phys. Rev. D40 (1989) 2184.

[24] L. F. Abbott *et al.*, Phys. Rev. D22 (1980) 582.

TABLE CAPTION

- - Table 1. Normalization factors obtained from a smooth global fit to the cross sections measured in the eight SLAC experiments. The E139 data, for example, must be multiplied by 1.008 to normalize them to those of E140. The first uncertainty is statistical and the second is systematic. Not shown are the overall normalization uncertainties, which are ± 0.021 for hydrogen and ± 0.018 for deuterium.

Table 1.

Experiment	Hydrogen Normalization	Deuterium Normalization
E49a ¹	$1.012 \pm 0.005 \pm 0.003$	$1.001 \pm 0.006 \pm 0.002$
E49b ²	0.981	$0.981 \pm 0.005 \pm 0.002$
E61 ³	$1.011 \pm 0.008 \pm 0.004$	$1.033 \pm 0.007 \pm 0.003$
E87 ⁴	$0.982 \pm 0.005 \pm 0.011$	$0.986 \pm 0.004 \pm 0.010$
E89a ⁵	$0.989 \pm 0.020 \pm 0.020$	$0.985 \pm 0.021 \pm 0.020$
E89b ⁶	$0.953 \pm 0.004 \pm 0.004$	$0.949 \pm 0.004 \pm 0.001$
E139 ⁷		$1.008 \pm 0.004 \pm 0.002$
E140 ⁸		1.000

FIGURE CAPTIONS

Fig. 1. Extracted values of $R^d - R^p$ averaged over Q^2 at each x . The dashed line is a prediction¹⁸ based on diquark formation for the Q^2 range from 6 to 10 (GeV/c)².

Fig. 2. Values of $R(x, Q^2)$ obtained in this analysis. Also shown are E140 results' and high- Q^2 measurements from $\mu - N$ and $\nu - N$ scattering.²⁰⁻²² The errors shown on all SLAC data do not include the ± 0.025 systematic uncertainty due to radiative corrections.

Fig. 3. The SLAC R data averaged over the Q^2 range from 5 to 10 (GeV/c)². The curves indicate various predictions for the x -dependence of R at a Q^2 of 7 (GeV/c)²; also shown for comparison is the best fit model- R^{fit} . Errors shown do not include the ± 0.025 systematic uncertainty due to radiative corrections.

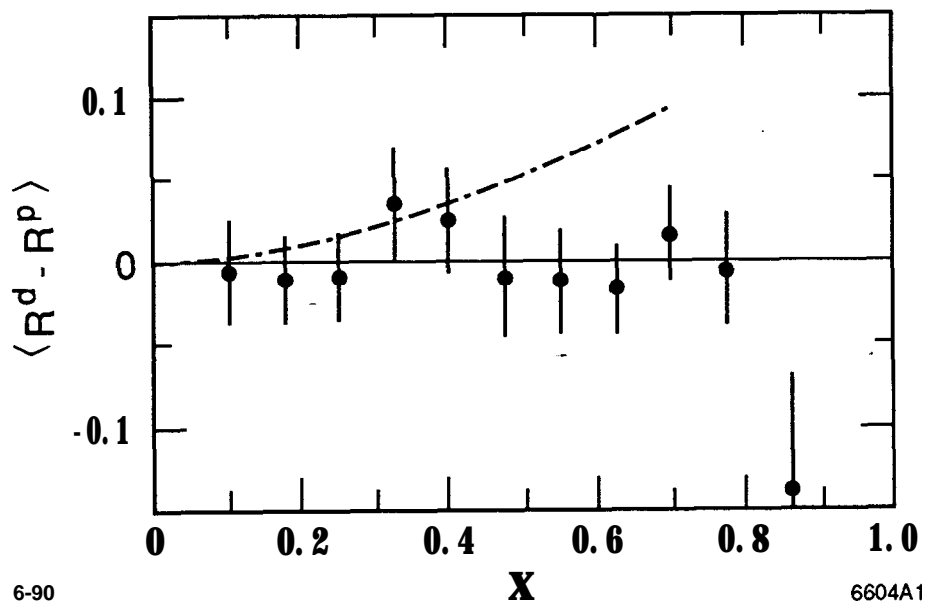


Fig. 1

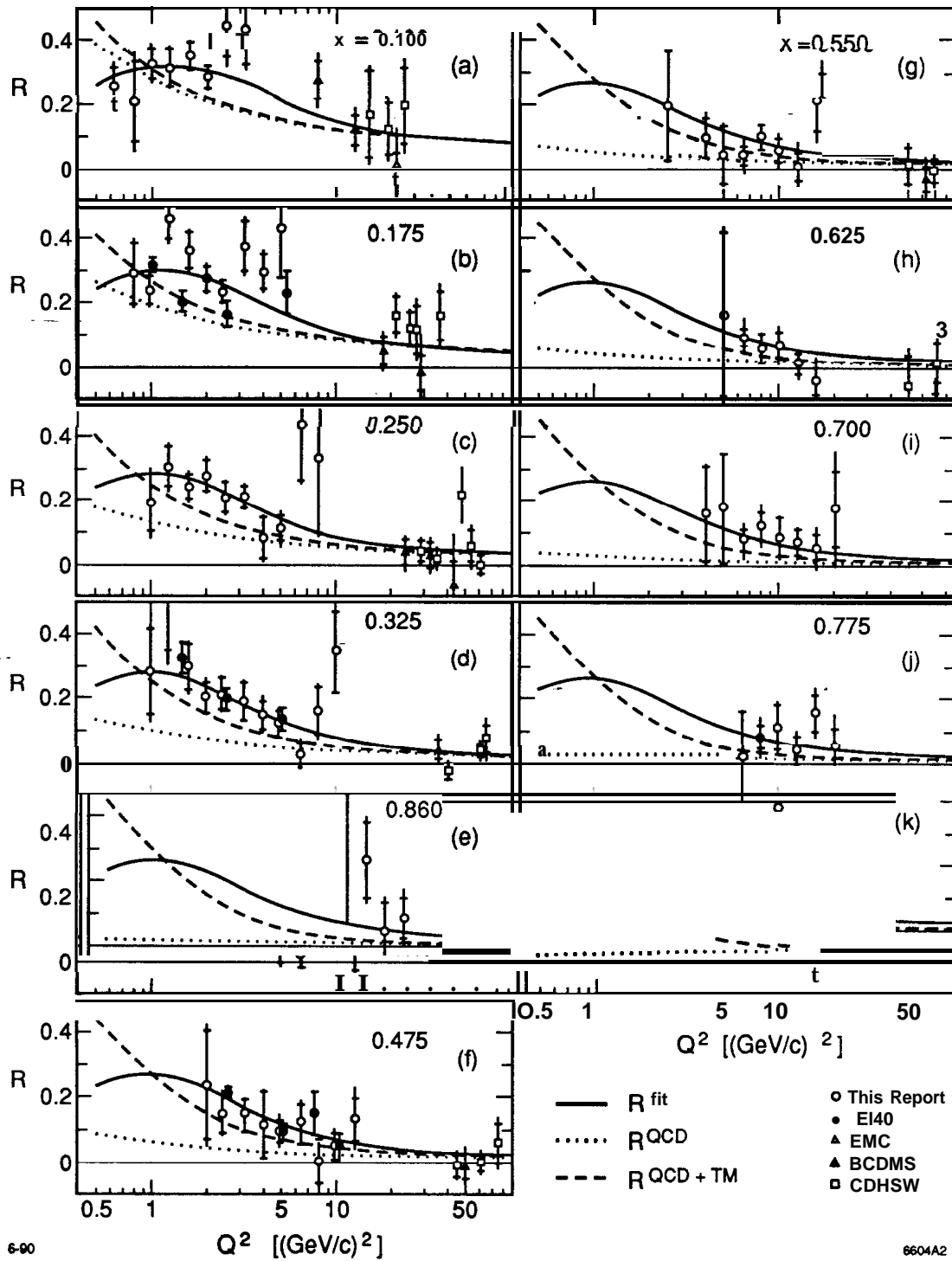


Fig. 2

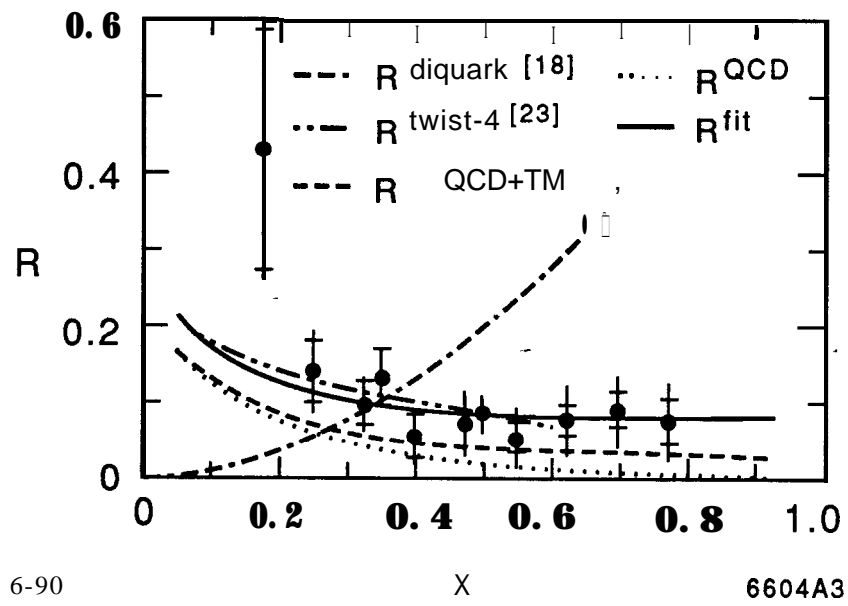


Fig. 3